Sub-picosecond Optical Damaging of Silica: Time Resolved Measurements of Light Induced Damage Threshold

Saulius Juodkazis,[b] Andrius Marcinkevičius,[b] Mitsuru Watanabe,[a] Vygantas Mizeikis,[b]
Shigeki Matsuo,[a] and Hiroaki Misawa[a]

[a]Department of Ecosystem Engineering, The University of Tokushima,
2-1 Minamijyosanjima, Tokushima 770-8506, Japan
[b]Laboratory of Nano-Photonic Materials, The University of Tokushima,
2-1 Minamijyosanjima, Tokushima 770-8506, Japan

ABSTRACT

We investigate damage of purified silica (transmission band down to 160 nm) by sub-ps light pulses having a wavelength of 795 nm. Illumination by 350 fs duration pulses focused by a high numerical aperture $NA = 1.35$ microscope objective results in one of the lowest reported values for the single-shot bulk light-induced damage threshold (LIDT) of 5 J/cm^2, well below the critical self-focusing power in silica. We have also investigated peculiarities of damage by two coincident laser pulses (duration 440 fs) having power of about $0.5 \times LIDT$, and linearly cross-polarized to avoid interference effects.
The reduction of LIDT in silica is demonstrated for an elevated lattice temperature T=400 K, at which the thermal linear/volume expansion coefficient has its maximum. Comparison between the LIDT values obtained from the numeric simulation and experiments demonstrates, that the critical density of optically generated free carriers corresponding to LIDT $n_{cr} \simeq 10^{21}$ cm^{-3} is reached during the first half time of the laser pulse illumination(0.2 ps).

Keywords: silica, time-resolved measurements, light-induced damage threshold, defects

1. INTRODUCTION

Reduction of a photo-modification threshold of materials is important in order to make femtosecond fabrication more practical and cost-effective. To achieve this goal, understanding of a light-material interaction dynamics on the time scale ranging from femtoseconds to nanoseconds is necessary. Numerous investigations of the interaction of intense laser radiation with transparent solids have focused on the dependence of the surface damage threshold on the pulsewidth in various materials,[1–3] while the role of multiphoton and avalanche ionization have been studied in.[4–6]

Dielectric breakdown through the optical absorption of the laser radiation is due to partial or complete ionization of the material, and is usually treated as a consequence of the following processes: i) the multiphoton ionization coupled with tunneling, causing the excitation of electrons into the conduction band, ii) the electron-electron collisional ionization due to the Joule heating, iii) plasma energy transfer to the lattice. In the first two processes, energy from the laser radiation is transferred to the free carrier plasma, while the third process releases plasma energy to the lattice, thus inducing permanent damage. Vaidyanathan *et al.*[7] emphasize that in many cases when ionization potential $\Delta \simeq 4\hbar\omega$, the strength of the damage field predicted by the Keldysh multiphoton absorption formula is smaller than that resulting from the avalanche model, and is in close agreement with the experimental value. Moreover, these observations are in consistent with Blombergen's[8] hypothesis, according to which the multiphoton absorption would be the dominant mechanism for the laser-induced damage for photon energies exceding half of the bandgap energy. Stuart *et al.*[4] has shown that if the multiphoton ionization occurs during the pulse propagation and the excited free electrons further seed the electron avalanche, the rate-equation approach can be used to obtain the electron density which determines the ablation threshold. Recent results confirm that this model of optical breakdown is valid in general, but the nature and relative role of the electron avalanche and photoionization still

Author information:
S.J. and V.M: On leave from: Institute of Material Research and Applied Science, Vilnius University, Sauletekio 10, Vilnius 2054, Lithuania, E-mail address of S.J.: saulius@svbl.tokushima-u.ac.jp
H.M.: Corresponding author. E-mail address: misawa@eco.tokushima-u.ac.jp

Laser-Induced Damage in Optical Materials: 2000, Gregory J. Exarhos, Arthur H. Guenther,
Mark R. Kozlowski, Keith L. Lewis, M. J. Soileau, Editors, SPIE Vol. 4347 (2001)

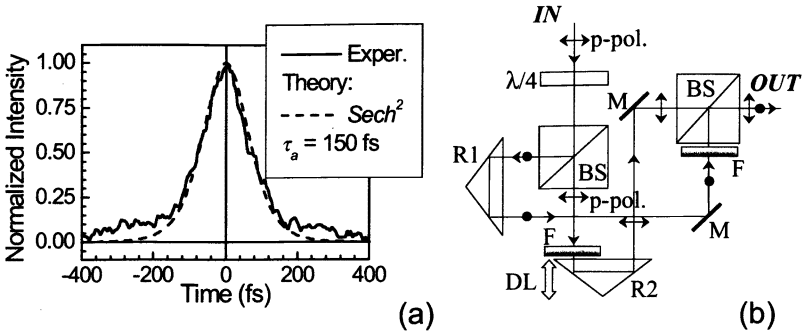

Figure 1. (a) The autocorrelation trace (obtained by second harmonic generation) of the laser pulse (solid line). The trace is fitted by assuming $Sech^2$ pulse shape (dashed line) with the pulse width of $\tau_p = \tau_a/1.543 = 97$ fs. (b) The setup for obtaining two separate delayed pulses for two-pulse LIDT measurements. R1 and R2 are the broadband hollow retro-reflectors. R2 is mounted on a high precision delay line DL with 2 fs resolution, M are the mirrors, F are the metallic variable neutral density filters, and $\lambda/4$ is the quarter-wave plate.

remain controversial. Also, it should be noticed that tunneling ionization can contribute to the free-carrier excitation, especially in the case of pulses shorter than ~100 fs. However, only few experimental and theoretical investigations were performed on the light-induced damage mechanism in the bulk of silica.[1,9,10] One of the possible reasons for this situation is that great care must be taken to avoid the self-focusing, which can significantly alter the experimentaly determined values of LIDT for subpicosecond pulses. The application of high numerical aperture microscope lens for the pulse focusing gives the possiblity to overcome this problem.[10,11] Such focusing conditions allow to reach a single-shot LIDT at much lower power level then in the case of self-focusing. The critical self-focusing power for the silica glass is about 3.92 MW, whereas the laser peak power in our experiments was just 0.74 MW even at 10×LIDT. Therefore, we do not need to take the self-focusing into account in the numeric simulations.

It is important to note, that fast (femtosecond) and slow (longer than ps) relaxation processes can be exploited to lower the photo-modification threshold in the experiments using two beam irradiation. In silica, both sub-ps (0.2 ps[12,13]) and extremely long ns-ms (lifetime of self-trapped exciton[14]) relaxations are reported. The second pulse can effectively launch an avalanche, which eventually reaches the light-induced damage threshold (LIDT or dielectric breakdown) of the material, provided that free carriers (electrons and holes) seeded by the first pulse, are present. The role of the holes in multiphoton absorption and in the avalanche formation has not been addresed properly so far. Recently it was demonstrated, that the decay of hole at O 2s level can generate two pairs of excitons in silica.[15]

In this work we report the reduction of LIDT in silica when two pulses are used for the damaging, and demonstrate the possibility to reduce LIDT by increasing the lattice temperature.

2. EXPERIMENTAL

The experimental setup for LIDT measurements consists of a Ti:sapphire laser with regenerative amplifier (Spectra Physics) and a microscope (Olympus IX70 or Nikon Otiphot-2). Typical pulse energy of the laser system is 0.5 mJ, duration 100-120 fs (FWHM) (Fig. 1(a)), and the central wavelength of 795 nm. The pulse is then split into two mutually delayed pulses using the setup shown in Fig. 1(b). The mechanical precision of the delay stage (500 nm) allows to achieve 2 fs temporal resolution, while broad delay range is ensured by the possibility to use coarse translation of the delay stage. The two pulses are introduced co-axially into the microscope, where they are focused by 100× magnification and $NA = 0.5 - 1.35$ numerical aperture objective lens into the constant 100 μm depth of the sample. We carefully estimated the temporal pulse spreading induced by the optical elements used in the setup. In our experiments we used polarizing beam splitters (BS in Fig. 1(b)) made from highly dispersive BK-7 optical glass. The eventual pulse duration at the entrance to the microscope is about 430 fs, while the microscope alone broadens the laser pulse to about 350 fs. Thus, the actual pulse duration at the irradiation site is about 440 fs in the two-pulse LIDT experiements.

The temporal coincidence of the pulses was checked using co-linear second harmonic generation in a 1 mm thick BBO crystal (I^{st} phase-matching type). The optical axis of the crystal was oriented at 45° with respect to the plane

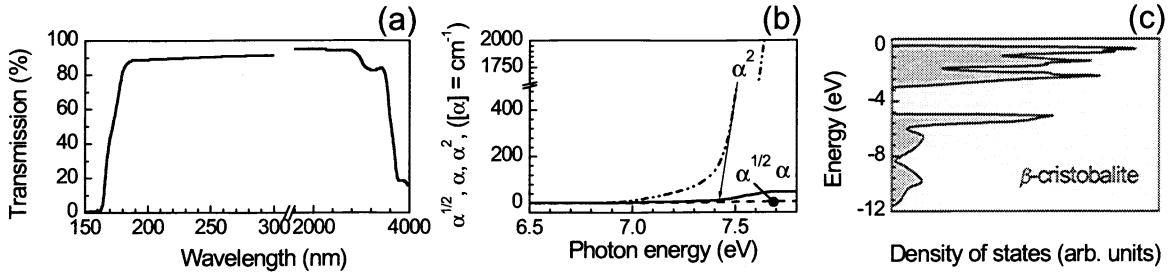

Figure 2. (a) The transmission spectrum of 10 mm thick plate of ED-C silica. (b) The evaluation of bandgap energy by $\alpha \propto \sqrt{h\nu}$ for allowed direct transitions and $\alpha \propto h\nu^2$ for indirect transitions. Here α is the absorption coefficient. (c) Valence band structure of β-cristobalite SiO_2 structure.[16]

of the incident beam polarization. This allowed to fix the temporal overlap of the two pulses to be less than 0.4 ps. Direct observation of the spatial (lateral and axial) coincidence of the two pulses by using the microscope was done by visualization of the focused beam luminescence in the rhodamine dye solution. The spatial coincidence was fixed with precision better than 0.3 μm. The spatial overlap of the two pulses was also checked by observing the damage by each pulse separately, i.e. at the power level of $LIDT$.

The temperature dependence of LIDT was measured using a Linkam-1500 annealing chamber mounted on the Nikon Optiphot-2 microscope. The setup allows to heat the sample up to the temperature of 1500°C, while irradiating and observing it using 40× magnification objective lens of $NA = 0.55$.

In our experiments we used low contamination silica, ED-C brand, from Nippon Silica Glass (OH concentration less than 1 ppm, Cl $\leq$ 830 ppm) with transmission band up to ca. 160 nm (transmission at 50% shown in Fig. 2(a)). Synthetic ED-C silica was made by a vapor-phase axial deposition (VAD), a kind of soot remelting technology. Effective bandgap of ED-C silica was evaluated from the dependence $\alpha \propto \sqrt{h\nu}$, which is valid for a direct transitions and yields Δ=7.4 eV (Fig. 2(b)). Such estimate assumes direct optical transitions occurring between the tails of density of states in amorphous materials. The valence band structure of β-cristobalite SiO_2 is shown in Fig. 2(c). The density of states in valence band of amorphous silica is in principle similar to that of β-cristobalite and is relevant to the consideration of hole "heating" by an absorption (similar to the well known electron "heating" in conduction band). The energy of the holes within the valence band can reach the value comparable to the silica bandgap.

3. RESULTS AND DISCUSSION

3.1. Definitions of Light Induced Damage Threshold (LIDT)

Large number of experimental and theoretical studies have been devoted to determine LIDT in various materials. The recent experimental data in silica are summarized in Table 1. The discrepancy seen in the experimental results may arise from the different techniques of LIDT determination. So far the most popular laser-induced damage definition techniques are: i) light scattering at the irradiation point, ii) plasma emission (white continuum generation), iii) observation of any visible permanent sample modifications with Nomarski-type microscope. Quoix *et al.*[19] have demonstrated the possibility to study the breakdown study by using frequency domain interferometry (FDI).

In our work determination of LIDT for the single pulse was done by direct *in situ* optical observation in the microscope with about 398 nm spatial resolution using $NA = 1.35$ objective lens (i.e. the lateral resolution attainable with condenser illumination of the fabricated spot). Hereinafter $LIDT(1)$ refers to the single pulse LIDT, whereas $LIDT(2)$ to the double pulse LIDT. LIDT was determined as the power level at which 75% of all laser shots leave observable change in the optical contrast in the sample. Having this definition enabled us to determine the LIDT values more than 2 times lower, compared to those reported by Du *et al.*.[1] The single-shot bulk LIDT fluence was 5 J/cm^2 for the 350 fs pulses (see Table 1). Taking into account that LIDT(1) value was typically by 30-40% larger than that for surface damage (ablation) threshold for different materials (silica, sapphire, rutile-TiO_2, and PMMA), we conclude that this definition of LIDT is precise, simple, and does not dependend on the sample surface quality and treatment.

Table 1. Dielectric breakdown thresholds in silica.

Pulse duration, fs	Wavelength, nm	F_{th}, J/cm^2	Detection method	Remarks	Source
20	780	2	Scattering	single-shot, surface	Ref. 2
25	800	1.5	Continuum generation	single-shot, surface	Ref. 12
100	800	3.9	Optical microscope	single-shot, bulk	Ref. 17
100	800	2.89	Scattering	multi-shot, bulk	
100	800	3.8	Nomarski microscope	single-shot, surface	Ref. 18
100	800	0.9	Nomarski microscope	multi-shot, surface	
150	825	1.8	Nomarski microscope	multi-shot, surface	Ref. 4
200	800	2	Nomarski microscope	Single-shot, surface	Ref. 3
200	800	11	Continuum generation	Single-shot, bulk	Ref. 1
760	800	1.7	FDI	Single-shot, surface	Ref. 19
350	795	5	Optical microscope	Single-shot, bulk*	Present study
350	795	4.5	Optical microscope	Multi-shot, bulk*	
440	795	6.9	Optical microscope	Single-shot, bulk*	

* Measured at 100 μm depth.

When the determination of $LIDT(N)$ is done for the multi-shot irradiation, $N > 1$, special attention must be paid to the spatio-temporal overlap of the pulses. Fig. 3 shows how consecutive irradiation of closely spaced locations may lead to "erasure" of the previously recorded neighboring bits. This is demonstrated by erasing the recorded bit by subsequent illumination (at $3 \times LIDT(1)$ fluence) of the spot separated by more than the diameter of the bit. The same phenomenon was observed at the fluencies approximately equal to $LIDT(1)$ if the spatial separation was less than the bit radius. Similar effect was reported when the optically recognizable bit was re-positioned by a multi-shot irradiation during the constant relocation of irradiation spot at the pulse repetition rate of 1 kHz.[20] Here we present the first report of a similar phenomenon induced by a single-shot irradiation. As far as the two-pulse irradiation is concerned, in determination of $LIDT(2)$, the pulse spatial overlap is essential, since mis-alignment can cause erasure, or at least, change the optical contrast of the recorded bit. This can be exploited to observe the dynamics of the micro-explosion if the distance between two or more pulses at the focal spot can be controlled. Fittinghoff *et al.*[21] have demonstrated the possibility of high resolution multifocal-multiphoton imaging in the optical microscope by introducing a slight mis-alignment between several beams at the entrance aperture of high-NA oil-immersion objective lens.

3.2. Two pulse damaging of silica

Is $LIDT(N > 1) < LIDT(1)$? If the first laser pulse with sub-threshold energy $E_1 < LIDT(1)$ modifies the material to a degree sufficient to change LIDT value, then the second pulse could in principle induce optical damage even at $E_2 < LIDT(1) - E_1$. This scenario was checked with two linearly cross-polarized fs-pulses. Cross-polarized irradiation allows to avoid interference effects, which may decrease the accuracy of the LIDT determination. In the two pulse experiments the energy of the first pulse E_1 was fixed at certain level below $LIDT(1)$, and in the following is expressed in the units of $LIDT(1)$, while the energy of the second delayed pulse E_2 was at each delay adjusted to

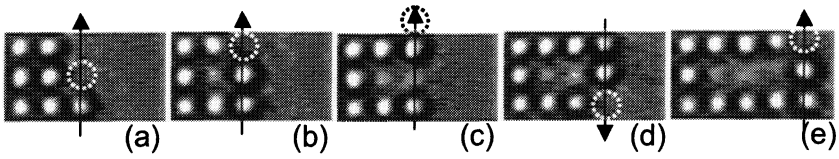

Figure 3. The series of consecutive images (a-e) during a single-shot recording by ca. 100 fs (at laser output) pulses at 795 nm wavelength in ED-C silica. The recording fluence was at the level of $3 \times LIDT(1)$. The arrows mark the direction of the laser beam positioning motion, and dashed circles show locations of the next irradiation spots.

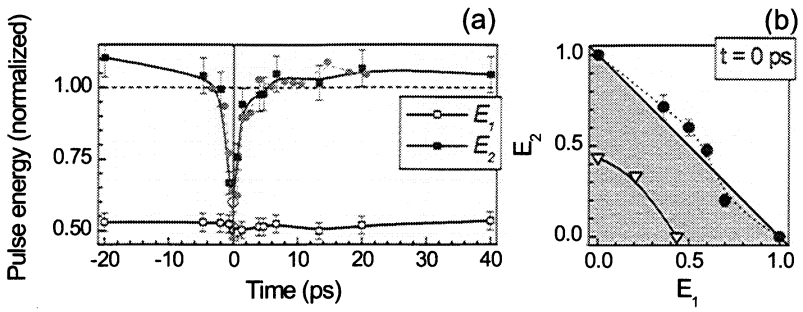

Figure 4. Optical damaging of ED-C silica with two fs-pulses separated in time. (a) The dependence of second pulse energy, E_2, on the time delay between the two pulses at different ratio E_2/E_1 ($E_1 = 0.5 \times LIDT(1)$ black and $E_1 = 0.4 \times LIDT(1)$ - grey markers). The energy of the first sub-threshold pulse, E_1, was constant. The pulse energies are normalized to the single-shot $LIDT(1) = 32.6$ nJ of silica. (b) Verification of the dependence $E_1 + E_2 = LIDT(1) \equiv 1$. The grey region depicts the area where $LIDT(2) < LIDT(1)$ in silica. The data on $LIDT(1)$ in sapphire is given by the triangles (normalized to the $LIDT(1)$ of silica). The lines are guides for the eye only.

the level required to reach the optical breakdown. For positive delays the fixed-energy pulse E_1 precedes the delayed one. The absolute value of LIDT(1) was found to be 6.9 J/cm^2.

The silica surface ablation experiments using double-pulse irradiation[12] have demonstrated sharp increase in LIDT for the second pulse within the delay range 67-200 fs. The energy two beam ratio was kept constant, while their energies were varied simultaneously (but always below the single pulse LIDT(1)) to reach LIDT. The obtained results were later explained by self-trapping of the electron-hole pairs and formation of self-trapped excitons.[22] In our experiments, we have observed similar increase in LIDT for the delayed beam, but for much longer delays between 1 and 2 ps (Fig. 4(a)). The actual pulse duration inside the sample is 440 fs. The first pulse at $0.5 \times LIDT$ creates certain density of free conduction electrons below the critical LIDT density (see Sect. 3.5 for details). The electron density peaks after about 300 fs, and decays at later times. The delayed pulse interacts with the excited free carriers, and thus less energy is required in order to reach the critical density at zero delay between the two pulses. With increasing delay, the electron density in left in the conduction band for interactions with the delayed pulse decreases due to relaxation (such as free-carrier scattering, fast nonlinear diffusion, all types of free-carriers capture and recombination), and therefore higher pulse energy is required for reaching LIDT. For long delays the material recovers totaly after the first pulse and one-pulse LIDT(1) is required for the damage.

The results in Fig. 4(a) shows that no decrease in LIDT(2) occurrs, i.e. $E_1 + E_2 = LIDT(1) \equiv 1$. Further

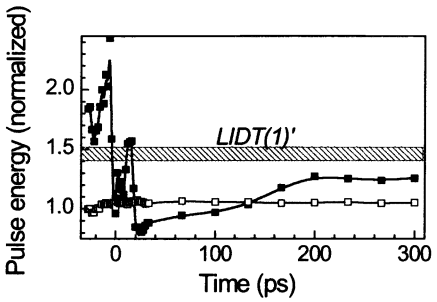

Figure 5. Optical damaging of ED-C silica with two axially offset fs pulses separated in time. The offset caused slight lateral shift (below our detection limit) of the focal spot inside the sample. The pulse energy is normalized to $LIDT(1) = 32.6$ nJ. The grey dashed area depicts the actual LIDT level of the particular experiment (marked as $LIDT(1)'$).

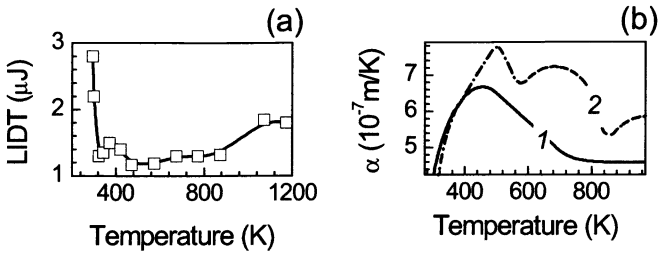

Figure 6. (a) The LIDT temperature dependence. The pulse energy is measured at the entrance of the microscope. The optical damage was inflicted using 40× objective lens with $NA = 0.55$. (b) Linear thermal expansion coefficient, α, of silica: fused (*1*) and synthetic (*2*) silica.

support of this conclusion is shown in Fig. 4(b), where the dependence of the delayed beam energy E_2 (required to reach $LIDT(2)$) on the fixed beam energy E_1 is shown. All data points were measured at zero delay between the pulses. Similar behaviour was observed even in the case of two pulse LIDT measurements in sapphire (Fig. 4(b)). Here $LIDT(1) = 0.43$ of that in silica (0001 plane of sapphire was irradiated at a 10 μm depth).

The data in Fig. 4 was obtained when the pulse spatial overlap and their alignment along the optical axis of the microscope were optimized. Under these conditions the lowest LIDT values were observed. The strongest source of uncertainty is beam misalignment which affects the axial overlap of the pulses. The signature of two pulses not coinciding spatially is the increase in the values of LIDT (marked as $LIDT(1)'$ in Fig. 5), also at negative delays. At negative delays the second pulse with $E_2 > LIDT(1)'$ irradiates the sample first, and is followed by the first pulse ($E_1 \simeq 0.7 \times LIDT(1)'$ in Fig. 5). One can expect that damage is due to the pulse which has arrived to the sample first, i.e. $E_2 > LIDT(1)'$ pulse. The results can be explained by the "erasing" phenomenon dicsussed in Sec. 3.1, which can only be observed when the two pulses do not precisely coincide at the focus. This explains the origin of the dip in E_2 at zero delay in Fig. 4, while the slow subnanosecond recovery in the E_2 can be explained by cooling of the irradiation spot. In contrast to the data shown in Fig. 4), the heating of the focal spot is more significant in this experiment, because the overall energy delivered to this spot is several times larger than that in the case of perfectly aligned setup. The influence of temperature on LIDT is discussed in the next section.

Finally, we note that deliberately introducing separation between the two focal points could be helpful in measuring the dynamics of microexplosions. For the typical sound velocity of 4.2 km/s in silica, 200 ps delay corresponds to a 84 nm distance in the sample.

3.3. Temperature dependence of LIDT

Fig. 6(a) shows how LIDT(1) in silica depends on the temperature. Decrease of LIDT by more than twice can be reached by moderately elevating the temperature to $150 - 250$°C. The temperature dependence of linear thermal expansion coefficient, α, of similar silica glasses is presented for comparison in Fig. 6(b). The obvious anti-correlation between $LIDT(T)$ and $\alpha(T)$ can be understood in terms of temperature dependencies of molar heat capacity at constant volume C_V and thermal conductivity, κ, (see discussion in the text).

The mechanical properties of materials related to the optical damage, such as linear thermal expansion coefficient, $\alpha(T) = L^{-1}dL/dT$ (L is the length in arbitrary units), and thermal conductivity, κ, are by definition temperature dependent. For isotropic glass material, the volume expansion coefficient $\alpha_V = 3\alpha$ and the Grüneisen relationship relates the thermal expansion coefficient to the molar heat capacity $\alpha(T) = \gamma C_V(T)/(3B_0V_0)$, where B_0 and V_0 are the bulk modulus and the volume at $T = 0$ K, respectively, and $\gamma = 1 \div 2$. Thus, α has the same temperature dependence as the heat capacity at constant volume C_V. The thermal conductivity is given by $\kappa = C_V vl/3$, where v is the phonon (sound) velocity and l is the mean free path of phonons. At low temperature ($T \ll \theta_D$, where θ_D is the Debye temperature of crystal) both α and κ rise as T^3 (Debye theory $C_V(T) \propto T^3$). At higher temperature C_V reaches classical limit $C_V(T) \Rightarrow const$. At the same time, $\kappa \propto 1/T$ at high temperature, since the phonon density is proportional to T an consequently $l \propto 1/T$.

The results in Fig. 6(a) show that optical damage of silica can be inflicted at lowest fluence when the linear thermal coefficient is maximized. Even for short pulses (< 1 ps) the temperature of target silica is important. As far

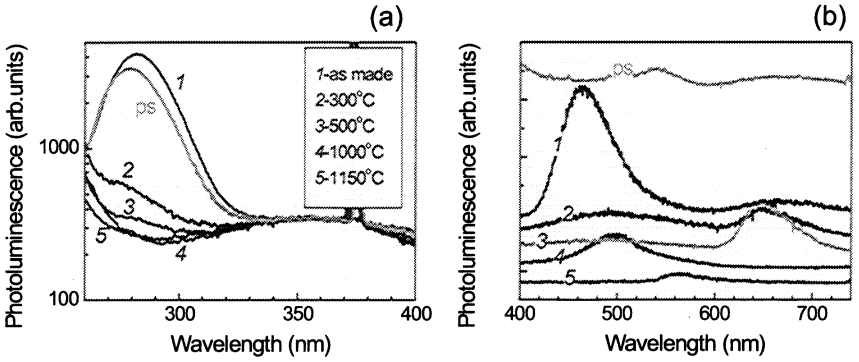

Figure 7. Photoluminescence of optically damaged silica excited by 250 nm illumination and annealed at different temperatures (given in the inset of (a)) in the range of 300-1150°C. The same sample was kept for 1 h at each temperature. Silica was optically damaged by fs-pulses at 795 nm by single pulse per damage. The pulse energy was 160 nJ ($LIDT(1) \simeq 33$ nJ). (a) PL spectra in the spectral region of oxygen vacancies at 280 nm and Cl related band at 360 nm. (b) Long-pass filtered PL (360 nm filter) of the same samples as in (a). The spectra are offset for clarity. *ps* marks the sample of the same ED-C silica optically damaged by ps-pulses in single shot at 174 nJ energy per pulse.

as optical damaging using high-NA objective is concerned, the fast melting and thermal quenching is important due to small volume of the excited material, usually 1 μm^3. The spatio-temporal profile of the temperature field after the excitation by δ-function thermal pulse is given by solution of the equation $\partial T/\partial t = \chi \Delta T + Const \times \delta(r)\delta(t)$, namely:[23]

$$T(r,t) = \frac{Const}{(4\pi\chi t)^{3/2}} \exp\left(-\frac{r^2}{4\chi t}\right), \tag{1}$$

where χ is the thermal conductivity, which can be expresed in terms of mass density, ρ, heat capacity at constant pressure, C_P, and thermal coductivity, κ, by $\chi = \kappa/\rho C_P$; r, t are spatial coordinate and time, respectively. This suggests that the irradiation spot is expected to cool down as in time according to the law $T \sim t^{-3/2}$, and spread according to the $r \sim (\chi t)^{1/2}$ law. The characteristic time d^2/χ shows the timescale scale over which the temperature changes are expected to occur at the irradiation spot of diameter d. For silica, $\chi = 8.408 \cdot 10^{-7}$ m^2/s, and taking the diffraction limited irradiation spot diameter $d = 1.22\lambda/NA = 718$ nm, one can find $d^2/\chi \simeq 610$ ns. Much faster changes were observed experimentally (Fig. 5) in the recovery of E_2. One possible explanation of these results is the nonlinear diffusion, and much smaller than expected diameter of the spot excited/heated by the first pulse.

3.4. Photoluminescence of ps- and fs-damaged silica

The properties of silica optically damaged by fs-pulses depend on the thermal treatment following the irradiation. Similarly, the thermally modified material will have different optical properties and LIDT (Sec. 3.3)after the fs damaging. This can be demonstrated by the PL spectra of silica illuminated by ps-pulses. The spectrum (marked as *ps* in Fig. 7) is similar to that of fs-irradiated silica annealed at T = 1050-1100°C.

The PL band at 280 nm is due to oxygen vacancies, V_O, created by the optical damaging. The absorption band of V_O is at 250 nm, and this wavelength was used for the excitation. The PL band at 650 nm is a signature of non-bridging oxygen hole center (NBOHC). The tendency of a red-shift with annealing in the 470 nm band (Fig. 7(b)) can be explained by the recombination of electron-hole pairs separated on the vacancy-interstitial, a Frenkel type pair of defects, i.e. V_O-$(O_2)_i$ as we have reported earlier.[24] The anealing alters the configuration of the defect pair; the diffusion of O_2 is thermally activated, and consequently, the PL is less intense and red-shifted.

3.5. Simulation of LIDT

In this part we are going to discuss mechanisms responsible for the electron promotion into the conduction band of silica under the excitation by 440 fs pulses. However, the determination of the optical breakdown threshold should be adressed in prior. From the modeling point of view, the optical breakdown of a dielectric is associated with the excitation of free carriers with density equal to or above the critical density n_{cr}, into the conduction band of the material. In a more rigorous theoretical approach the breakdown is assumed to occur above the critical laser intensity (or laser field [V/cm]) when the rate of the electron energy gain from the laser field exceeds the rate of the energy loss to the lattice by the phonon scattering; or when the solid reaches the temperature close to the melting (or softening for glasses) point.[25] In our calculations we use free electron density 10^{21} cm^{-3}, which is close to the plasma frequency for 795 nm iradiation: $n_{cr} = \omega^2 m\epsilon_0/e^2 = 1.4 \times 10^{21}$ cm^{-3} , where ω is the laser angular frequency, m is the electron mass, ϵ_0 is the vacuum permitivity, and e is the electron charge. Referring to the LIDT definition given in Sect. 3.1, such silica modification exhibits signatures of very hot and dense plasma formation accompanied by the microexpolsion at the beam focus. During the pulse propagation both plasma excitation and heating must occur. Therefore, we will use $\tau_p/2$ as an estimated breakdown time (the carrier density n_{cr} is reached), regardless of whether cascade or multiphoton ionization is the dominant mechanism.

For the numeric modeling of the change in the free electron density we use modified rate equation formalism derived by Stuart *et al.*.[4] Based on the transmission spectrum (Fig. 2(b)), we take the ionization potential of the ED-C brand silica to be 7.4 eV instead of commonly accepted bandgap energy of crystalline quartz silica $\Delta \simeq 9 \div 10$ eV. The photo-ionization is sensitive to the Keldysh parameter $\gamma = \omega\sqrt{m^*\Delta}/eE$, which conditionally divides the ionization process into two types: the multiphoton ionization when $\gamma \gg 1$, and the tunneling ionization when $\gamma \ll 1$; here E is the peak laser field, and $m^* = 0.8m$ is the reduced electron mass (see eqn.8 in Sec.A). The numeric calculations are most complex for $\gamma \sim 1$, when the simplifications made in the expression for the dielectric ionization probability for tunneling or multiphoton ionization are no longer valid. Under our experimental conditions Keldysh parameter varies as $\gamma = (1.1 \ldots 1.8)$. We would like to point out, that some papers deling with dielectric breakdown do not pay attention to the importance γ value, which is also sensitive to such material constants as the effective mass of electron and the bandgap energy. We used the following Keldysh expression for the probability of the multiphoton ionization in condensed matter[26]:

$$W = \frac{2}{9\pi}\omega\left(\frac{m^*\omega}{\hbar}\right)^{\frac{3}{2}} \exp(2K)\Phi(z)\left(\frac{1}{16}\right)^K \left[\frac{e^2 I_0}{m^*\Delta\omega^2 c\varepsilon_0 n_0}\right]^K \tag{2}$$

$$\Phi(z) = \exp(-z^2)\int_0^z \exp(y^2)dy \tag{3}$$

$$z = \sqrt{2K - \frac{2\Delta}{\hbar\omega}}, \tag{4}$$

here $K = \langle 1 + \Delta/\hbar\omega \rangle$ is the number of photons necessary to ionize silica. Using this expression the six-photon ($K = 6$) ionization rate *P(I)* can be expressed as

$$P(I) = 4.07 \times 10^{13} I_0^6 \text{ cm}^{-3}\text{ps}^{-1}, \tag{5}$$

where the peak intensity I_0 is in TW/cm^2. This value is about 3 orders of magnitude lower than that quoted in Ref. 19, but about 5 orders of magnitude exceeds that reported by Lenzner *et al.*.[2] However, it is worthwhile to note, that smaller ionization rate assumed in our calculations does not change the qualitative picture of the interplay between the multiphoton and cascade ionization (the tunneling ionization is less important for less intense light fields).

Once free electrons are promoted into the conduction band by multiphoton absorption, they can further gain energy by single photon absorption similar to so called inverse bremsstrahlung absorption in the ionized gas. The highly energetic electrons undergo momentum and energy relaxation simultaneous with absorption, during which the electron-electron and electron-phonon collisions can be assumed to be inelastic, and new electron-hole pair is created in every collision. The cascade ionization rate α per electron is given by:[27]

$$\alpha(I) = \frac{1}{\omega^2\tau^2 + 1}\left[\frac{e^2\tau}{cn\varepsilon_0 m\Delta} I_0\right], \tag{6}$$

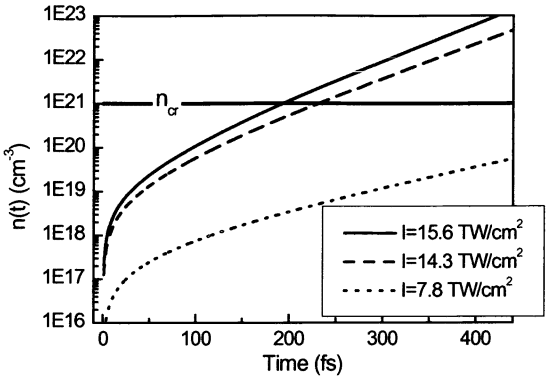

Figure 8. The dependence of the excited free electron density on the excitation time (Eqn. 7), showing the effect of the laser irradiation intensity on the temporal profile of the free electron density. The critical plasma density, n_{cr} corresponds to the optical breakdown of silica. The laser pulse duration is 440 fs (FWHM).

here τ is the effective electron collision time, n is the silica refractive index. In our calculations we took $\tau = 2$ fs.[28] Therefore, minimum time for each doubling sequence in the avalanche is given by the product $\tau \times K = 12$ fs. If every inelastic collision is coupled with the inverse bremsstrahlung event, a cascade starting from a single seeded electron can produce $2^{440/12} = 1.4 \times 10^{11}$ free electrons in one laser pulse. This implies that the free electron density of 10^{10} cm^{-3} must be produced by multiphoton ionization to finally reach the critical electron density ρ_{cr} by avalanche. Eqns. (6) and (5) can be combined into the following expression for a conduction band electron density:[4]

$$n(t) = \left(n_{c0} + \frac{P(I)}{\alpha(I)}\right) \exp\left(\alpha(I)t\right) - \frac{P(I)}{\alpha(I)}, \tag{7}$$

where n_{c0} is the initial free electron density in the conduction band. Using this expression we can predict the electron density $n(t)$ excited during a passage of $\tau_p = 440$ fs pulse, and $\omega = 2.37 \cdot 10^{15}$ s^{-1} frequency for fixed irradiation intensity. Fig. 8 shows the temporal evolution of the free electron density following the excitation by a fs light pulse for different intensity levels: the experimentally obtained $LIDT(1)$ (solid line), the theoretical $LIDT(1)$ value considering the breakdown is reached at the half of the pulse (dashed line), and $0.5 \times LIDT(1)$ (dotted line). It follows from the theoretical calculations, that at the experimentally determined LIDT (15.6 TW/cm^2) the breakdown occurs during the first 192 fs, while the theoretical LIDT intensity is 14.3 TW/cm^2. The linear dependence of the free electron density on time in a semi-logarithmic plot in Fig. 8 proves that the optical breakdown is initiated by the multiphoton ionization, which is followed and eventually completed by the cascade ionization if the pulse duration is about 0.5 ps, and the latter mechanism is more important than the multiphoton ionization. Returning to the double pulse measurements, we have checked the density of free electrons which can be excited by $0.5 \times LIDT$ intensity pulse (See Fig. 8). Our simulations yield 4.5×10^{18} cm^{-3} during the first 220 fs and about 5.6×10^{19} cm^{-3} within the entire 440 fs pulse. The resulting electron density is only two orders of magnitude smaller than the critical density. It follows from this, that intensity of the second pulse smaller than $0.5 \times LIDT$ is needed to reach the critical density ($LIDT(1)$ level). However, our experimental results in Fig. 4(a) show that the energy of the second pulse was higher than required $0.5 \times LIDT$ to reach $LIDT(1)$. This can be explained by the circumstance that the model neglects change in the refractive index experienced by the second pulse, and disregards some other processes leading to the free carrier losses, like recombination and diffusion at the focal spot. Taking into account small dimensions of the photoexcited volume, diffusion over the distances ranging from tens to hundreds of nm may be strongly pronounced.

Absorption by free holes is another important factor not considered in this model, basicaly due to lack of data. As can be seen from the valence band structure shown in Fig. 2(c), the holes can be heated to the energies sufficient for the impact ionization. However, simulations give correct qualitative picture of an optical breakdown, and the experimentally observed values of LIDT are corroborated numerically.

4. CONCLUSIONS

Based on the investigation of LIDT in bulk silica by sub-picosecond light pulses we conclude that: i) focusing of 350 fs pulses by a high-NA microscope objective lens results in one of the lowest reported values for the single-shot bulk LIDT, 5 J/cm^2, well below the critical self-focusing power in silica; ii) the decay of the free-electron plasma excited by 440 fs pulses is approximately exponential with the time constant of 2 ps, much longer than reported by Li *et al.*[12]; iii) the single-shot LIDT decreases with increase of silica lattice temperature to about 400 K, at which the linear thermal expansion coefficient is at maximum; iv) the photoluminescence spectra of silica optically damaged by ps-pulses is similar to that of fs-irradiated silica annealed at about 1050-1100°C.

These findings allow to anticipate a decrease of LIDT for the second pulse in two pulse experiments when local heating or sufficient density of unrelaxed free carriers persist after the excitation by the first pulse with sub-threshold intensity till the arrival of the second pulse.

Moreover, we have demonstrated for the first time the single-shot "erasure" (decrease of the contrast in the optical transmission) of bits recorded previously by a single shot.

5. APPENDICES

APPENDIX A. EFFECTIVE MASS OF FREE ELECTRON IN SILICA

The effective mass, m^*, of the conducting band electron in silica can be evaluated using formulas derived from the perturbation theory $k{\cdot}p$ approach:[16]

$$\frac{m}{m^*} = 1 + \frac{2\gamma^2 m d^2 V_2^2}{3\Delta\hbar^2}, \tag{8}$$

where the covalent energy $V_2 = 2.16\hbar^2/(md^2)$. Here m is the electron mass, $d = 1.61$ Åis the length parameter for silica,[16] $\Delta = 7.4$ eV is the band gap energy, and scale parameter $\gamma \simeq 1$. This gives $m^* \simeq 0.8m$.

ACKNOWLEDGMENTS

This work was in part supported by the Satellite Venture Business Laboratory of the University of Tokushima.

REFERENCES

1. D. Du, X. Liu, G. Korn, J. Squier, and G. Mourou, "Laser-induced breakdown by impact ionization in SiO_2 with pulse widths from 7 ns to 150 fs," *Appl. Phys. Lett.* **64**, pp. 3071–3073, 1994.
2. M. Lenzner, J. Kruger, S. Sartania, Z. Cheng, C. Spielmann, G. Mourou, W. Kautek, and F. Krausz, "Femtosecond optical breakdown in dielectrics," *Phys. Rev. Lett.* **80**, pp. 4076–4079, 1998.
3. A. C. Tien, S. Backus, H. Kapteyn, M. Murnane, and G. Mourou, "Short-pulse laser damage in transparent materials as a function of pulse duration," *Phys. Rev. Lett.* **82**, pp. 3883–3886, 1999.
4. B. C. Stuart, M. D. Feit, S. Herman, A. M. Rubenchik, B. W. Shore, and M. D. Perry, "Nanosecond to femtosecond laser induced breakdown in dielectrics," *Phys. Rev. B* **53**, pp. 1749–1441, 1996.
5. B. C. Stuart, M. D. Feit, A. M. Rubenchik, B. W. Shore, and M. D. Perry, "Laser-induced damage in dielectrics with nanosecond to subpicosecond pulses," *Phys. Rev. Lett.* **74**, pp. 2248–2251, 1995.
6. T. Apostolova and Y. Hahn, "Modelling of laser-induced breakdown in dielectrics with subpicosecond pulses," *J. Appl. Phys.* **88**, pp. 1024–1034, 2000.
7. A. Vaidyanathan, T. W. Walker, and A. H. Guenther, "The relative roles of avalanche multiplication and multiphoton absorbtion in laser-induced damage in dielectrics," *IEEE J. Quantum Electron.* **16**, pp. 89–93, 1980.
8. N. Bloembergen, "Laser-induced electric breakdown in solids," *IEEE J. Quantum Electron.* **10**, pp. 375–386, 1974.
9. E. N. Glezer and E. Mazur, "Ultrafast-laser driven micro-explosions in transparent materials," *Appl. Phys. Lett.* **71**, pp. 882–884, 1997.
10. M. Watanabe, H. Sun, S. Juodkazis, T. Takahashi, S. Matsuo, Y. Suzuki, J. Nishii, and H. Misawa, "Three-dimensional optical data storage in vitreous silica," *Jpn. J. Appl. Phys.* **37**, pp. L1527–L1530, 1998.
11. H. Misawa, H. B. Sun, S. Juodkazis, M. Watanabe, and S. Matsuo, "Microfabrication by femtosecond laser irradiation," *Proc. SPIE* **3933**, pp. 246–260, 2000.
12. M. Li, S. Menon, J. P. Nibarger, and G. N. Gibson, "Ultrafast electron dynamics in femtosecond optical breakdown in dielectrics," *Phys. Rev. Lett.* **82**, pp. 2394–2397, 1999.
13. P. Martin, S. Guizard, P. Daguzan, and G. Petite, "Subpicosecond study of carrier trapping dynamics in wide-band-gap crystals," *Phys. Rev. B* **55**(9), pp. 5799–5810, 1997.
14. K. Shimakawa, A. Kolobov, and S. R. Elliott, "Photoinduced effects and metastability in amorphous semiconductors and insulators," *Adv. Phys.* **44**(6), pp. 475–588, 1995.

15. N. Matsunami and H. Hosono, "Bi-self-trapped-exciton model for frenkel defect formation in amorphous SiO_2 by proton irradiation," *Phys. Rev. B* **60**(15), pp. 10616–10619, 1999.
16. W. A. Harrison, *Electronic structure and the properties of solids. The physics of the chemical bond.*, ch. 11, Mixed tetrahedral solids, pp. 257–288. Dover Publications, Inc., 1989.
17. C. B. Schaffer, N. Nishimura, and E. Mazur, "Thresholds for femtosecond laser-induced breakdown in bulk transparent solids and water," in *Time structure of X-ray sources and its applications*, A. K. Freund, H. P. Freund, and R. M. Howells, eds., *Proc. SPIE* **3451**, pp. 2–8, 1998.
18. D. Ashkenasi, M. Lorenz, R. Stoian, and A. Rosenfeld, "Surface damage threshold and structuring of dielectrics using femtosecond laser pulses: the role of incubation," *Appl. Surf. Sci.* **150**, pp. 101–106, 1999.
19. C. Quoix, G. Grillon, A. Antonetti, J.-P. Geindre, P. Auderbert, and J. C. Gauthier, "Time-resolved studies of short pulse laser-produced plasmas in silicon dioxide near breakdown threshold," *Eur. Phys. J. AP* **5**, pp. 163–169, 1999.
20. W. Watanabe, T. Toma, K. Yamada, J. Nishii, K.-I. Hayashi, and K. Itoh, "Observation of voids and optical seizing of voids in silica glass with infrared femtosecond laser pulses," in *Proc. of Ist Int. Symp. on Laser Precision Microfabrication LPM2000, Jun.14-16, 2000, Omiya, Japan*, 2000 (In press).
21. D. N. Fittinghoff and J. A. Squier, "Time-decorrelated multifocal array for multiphoton microscopy and micromachining," *Opt. Lett.* **25**, pp. 1213–1215, 2000.
22. G. Petite, S. Guizard, P. Martin, and F. Quere, "Comment on "Ultrafast electron dynamics in femtosecond optical breakdown of dielectrics"," *Phys. Rev. Lett.* **83**, p. 5182, 1999.
23. N. I. Koroteev and I. L. Shumai, "Physics of intense laser radiation," *Nauka, Moscow* , 1991 (In Russ.).
24. M. Watanabe, S. Juodkazis, H. Sun, S. Matsuo, and H. Misawa, "Luminescence and defect formation by visible and near-infrared irradiation of vitreous silica," *Phys. Rev. B* **60**(14), pp. 9959–9963, 1999.
25. D. Arnold and E. Cartier, "Theory of laser-induced free-electron heating and impact ionization in wide-band-gap solids," *Phys. Rev. B* **46**, pp. 15102–15115, 1992.
26. L. V. Keldysh, "Ionization in the field of a strong electromagnetic wave," *Sov. Phys. JETP* **20**, pp. 1307–1314, 1965.
27. P. K. Kennedy, "A first-order model for computation of laser-induced breakdown thresholds in ocular and aqueous media: part I- theory," *IEEE J. Quantum Electron.* **31**, pp. 2241–2249, 1995.
28. P. P. Pronko, P. A. VanRompay, C. Horvath, F. Loesel, T. Juhasz, X. Liu, and G. Mourou, "Avalanche ionization and dielectric breakdown in silicon with ultrafast laser pulses," *Phys. Rev. B* **58**, pp. 2387–2390, 1998.